Robust Parameter Design Based on Functional Latent Gaussian Processes and Its Application in Additive Manufacturing

Yuancheng An, Mengchao Tu, Ruxin Bai, Ziyu Fan, Yanyan Pang *

School of Nanjing University of Science and Technology, Nanjing, China

* Corresponding Author Email: pangyanyanjg @163.com

Abstract. For the robust parameter design problem of functional responses, a novel robust parameter optimization model is proposed within the functional latent Gaussian process (LFGP) modeling framework. First, maximum likelihood estimation is employed to obtain the required hyperparameters for fitting the LFGP model. Second, leveraging the characteristics of the LFGP model, we construct an objective function that fully accounts for response variability, thereby establishing an optimization model for functional responses. Finally, we employ a genetic algorithm (GA) for global optimization to obtain optimal input parameter settings. Results from an additive manufacturing case study demonstrate that this method achieves superior prediction accuracy and optimization performance for functional data compared to traditional Gaussian process functional regression and principal component analysis models.

Keywords: Gaussian Process, Robust Parameter Design, Functional Response, Additive Manufacturing.

1. Introduction

In complex manufacturing and engineering systems, outputs are often presented as functions, termed functional responses, which frequently vary with spatial position, time points, or angular variables. For instance, in 3D printing—an advanced additive manufacturing technology [1] —the mechanical properties of printed products are not merely individual observations measured under each experimental condition. Instead, they are captured as curves measured at different times or positions along independent variables during each experimental run. This "functional response" is also termed a "profile response." Extracting meaningful insights from collected functional data offers unique opportunities for quality improvement. For products requiring specific shapes or performance characteristics, controlling these random variations over time or space is crucial to achieving defined quality targets. However, designing efficient metamodeling and robust parameter design (RPD) methods for such high-dimensional functional data presents an emerging research challenge.

Response Proportional Design (RPD) is one of the key technologies for achieving product quality improvement, first introduced by Dr. Genichi Taguchi [2]. It can effectively enhance product quality and increase economic benefits [3]. Given the shift in our focus from static single responses to functional responses, the scope of RPD research has gradually expanded from static single-response systems to functional response systems [4]. However, such responses are not only high-dimensional but also exhibit significant spatial correlation. Most studies employing traditional response surface models struggle to effectively address these robust parameter design challenges. To maximize "usefulness" and minimize "error," Gaussian processes (GP) have been selected from numerous models as a fast approximation for computationally intensive simulators. GP can approximate computationally expensive functions using finite samples, effectively reducing computational costs while maintaining simulation optimization accuracy, making it the preferred method for handling functional data modeling problems [5].

Numerous scholars worldwide have conducted extensive work on such meta-modeling problems, developing various GP-based functional response models. Early research on functional response surrogate modeling aimed to develop Gaussian Process Function Regression (GPFR) models by incorporating function parameters as additional inputs to the surrogate model [6, 7]. However, such

models often suffer from the curse of dimensionality. To overcome these limitations, some researchers introduced modeling approaches based on separable covariance matrices [8--[10]. For instance, Melkumyan et al. [11] proposed modeling outputs using non-separable covariance structures. This approach significantly enhances model flexibility by assigning independent covariance parameters to different output levels. To optimize covariance function selection, Li et al. [12] further developed a multivariate random field test method, providing a theoretical basis for determining covariance function separability. Beyond constructing separable covariance matrices, numerous researchers have developed models by reducing the dimensionality of functional responses.

For instance, Chung and Kontar [13] proposed a functional principal component approach for modeling functional responses on irregular grids; Sung et al. [14] introduced a multiresolution functional variance analysis model, a computationally efficient method suitable for multi-input, high-dimensional scenarios. Furthermore, Chen et al. [15] applied Gaussian processes to model high-dimensional outputs with spatiotemporal correlation structures, enhancing both model uncertainty quantification and prediction accuracy. Within Gaussian process-based functional response modeling, two-stage methods have recently gained attention for their flexibility in representing functional responses. Castillo et al. [16] proposed a two-stage mixed-effects regression model within a Bayesian framework, determining optimal parameter combinations by maximizing the probability that responses meet specification limits. Two-stage methods effectively represent functional responses under both regular and irregular grid conditions, balancing computational efficiency with model flexibility [17, 18].

However, when confronting highly nonlinear functional responses, such methods still face challenges: projecting functional data onto low-dimensional feature spaces may result in significant information loss[17, 19] , and the assumption of independence among feature variables may overlook the inherent spatial dependencies in functional outputs [18, 21]. This spatial correlation within the output domain is a critical factor in functional response modeling; neglecting it often leads to a significant decline in predictive performance.

2. Functional Response Gaussian Process Model

2.1. B-spline Parameterization of Functional Response

Let the observed spatio-temporal dataset be $\boldsymbol{y}_i = [y(\boldsymbol{x}_i, t_{i,1}), y(\boldsymbol{x}_i, t_{i,2}), ..., y(\boldsymbol{x}_i, t_{i,m})]^T$, where each input $\boldsymbol{x}_i$ is collected at different output locations $\boldsymbol{t}_i = \{t_{i,1}, t_{i,2}, .., t_{i,m}\}$, for $i = 1, 2, ..., n$. Due to the "curse of dimensionality" problem in directly modeling high-dimensional functional responses, we first introduce B-spline basis functions for parameterization.

B-spline basis functions are widely used in numerical analysis, and their construction depends on a knot vector and the polynomial degree. Let $\mathbf{U} = \{u_0, u_1, ...u_m\}$ be a non-decreasing real sequence, where u_i are called knots, and $\mathbf{U}$ as a whole constitutes the knot vector. Let $b_{i,p}(u)$ denote the i B-spline basis function of degree p (corresponding to order $p+1$). Its definition follows the Cox-de Boor formula:

$$b_{i,0}(u) = \begin{cases} 1 & u_i \le u \le u_{i+1} \\ 0 & otherwise \end{cases}$$
$$b_{i,p}(u) = \frac{u - u_i}{u_{i+p} - u_i} b_{i,p-1}(u) + \frac{u_{i+p+11} - u}{u_{i+p+1} - u_{i+1}} b_{i+1,p-1}(u), \tag{1}$$

From the above definition, calculating a set of B-spline basis functions requires pre-determining the knot vector $\mathbf{U}$ and the degree p . For example, given a knot vector $\mathbf{U} = \{0, 1, 2, 3\}$, the B-spline basis functions of different degrees can be calculated step-by-step according to the formula. For the

0-degree basis function, $b_{0,0}(u)$ is 1 only in the interval $[0,1)$ and 0 in other intervals. As the degree increases, such as when calculating the 1st-degree basis function $b_{0,1}(u)$, it is necessary to combine $b_{0,0}(u)$ and $b_{1,0}(u)$ using the formula.

B-spline basis functions have properties that provide strong support for the parameterization of functional responses. On one hand, they have local support, meaning if $u \notin (u_i, u_{i+p+1})$, then $b_{i,p}(u) = 0$. This implies that outside a specific interval, the basis function's value is always 0, greatly reducing interference between functions. In any given knot interval (u_i, u_j), at most $p+1$ $b_{i,p}$ functions are non-zero, further highlighting their local nature. On the other hand, B-spline basis functions are non-negative, for all $i, p, b_{i,p}(u) \geq 0$, ensuring that the coefficient combinations have good mathematical properties when constructing the functional response model. Using B-spline basis functions, the functional response $y(\boldsymbol{x}, t)$ can be expressed as follows:

$$y(\boldsymbol{x}, t) = \boldsymbol{f}(\boldsymbol{x})^T \boldsymbol{\beta} + \boldsymbol{b}(t)^T \boldsymbol{z}(\boldsymbol{x}) + \varepsilon(t), \tag{2}$$

Where $f(x) = [f_1(x), f_2(x), ..., f_q(x)]^T \in \mathbb{R}^q$ is the regression function, $\beta = [\beta_1, \beta_2, ..., \beta_q]^T \in \mathbb{R}^q$ is the regression coefficient, $\boldsymbol{b}(t)$ is composed of B-spline basis functions, and $\varepsilon(t) \sim \mathcal{N}(0, \sigma^2 \delta^2)$ is the measurement error term. $z(x) = [z_1(x), z_2(x), ..., z_k(x)]^T \in \mathbb{R}^k$ actually refers to the control points of the B-spline basis. They are spatially correlated, which is because the functional responses they represent are spatially correlated. Therefore, $\boldsymbol{z}(\boldsymbol{x})$ is treated as a latent variable to account for the underlying randomness of the functional response $y(\boldsymbol{x}, t)$ and follows a zero-mean MGP (Multivariate Gaussian Process) with the following covariance function:

$$Cov\left(z_r(\boldsymbol{x}), z_t(\boldsymbol{x})\right) = \sigma^2 \phi_0(r, t) \phi(\boldsymbol{x}, \boldsymbol{x}'), \; r, t = 1, ..., k. \tag{3}$$

The correlation in (3) consists of two parts. Wherein, $\phi(\boldsymbol{x}, \boldsymbol{x}')$ is the correlation kernel function between inputs $\boldsymbol{x}$ and $\boldsymbol{x}'$, here we use the squared exponential kernel:

$$\phi(\boldsymbol{x}, \boldsymbol{x}') = \exp\left(-\sum_{i=1}^{p} \theta_i \left(x_i - x_i^{'} \right)^2 \right), \tag{4}$$

And $\phi_0(r, t)$ is used to measure the correlation between the B-spline coefficients $\boldsymbol{z}_r(\boldsymbol{x})$ and $\boldsymbol{z}_t(\boldsymbol{x})$, also using a squared exponential kernel:

$$\phi_0(r, t) = \exp\left(-\theta_0 \sin^2\left(\frac{\pi(r-t)}{k-1} \right) \right). \tag{5}$$

In this paper, we assume that the spatial arrangement of $\boldsymbol{z}(\boldsymbol{x})$ corresponding to each input $\boldsymbol{x}$ remains consistent. Therefore, based on the functional response representation in Equation (2) and the correlation of the latent variable $\boldsymbol{z}(\boldsymbol{x})$, we introduce the Latent Functional B-spline (LFBS) kernel function as follows:

$$\psi_{\boldsymbol{\theta}}\left(y(\boldsymbol{x}, t), y(\boldsymbol{x}', t') \right) = \phi(\boldsymbol{x}, \boldsymbol{x}') \boldsymbol{b}(t)^T \boldsymbol{\Sigma}_z \boldsymbol{b}(t)^T + \delta^2 I_{t=t'}, \tag{6}$$

Where $\boldsymbol{\Sigma}_z = \{\phi_0(r, t)\}_{r,t=1,...,k}$ is the k times k correlation matrix, $\boldsymbol{\theta} = \{\theta_0, \theta_1, .., \theta_p\}$ are the correlation parameters for $\phi(\boldsymbol{x}, \boldsymbol{x}')$ and $\phi_0(u, v)$, δ^2 is the correlation constant for measurement error, and $I_{t=t'}$ is an indicator function; if $t = t'$, $I_{t=t'}$ equals 1, otherwise it equals 0.

2.2. Model Parameter Estimation and Efficient Optimization

In the functional response model, assume that the functional response $\boldsymbol{y}_i = [\boldsymbol{y}(\boldsymbol{x}_i, t_{i,1}), ..., \boldsymbol{y}(\boldsymbol{x}_i, t_{i,1})]^T \in \mathbb{R}^m$ is collected at locations $\boldsymbol{t}_i = \{t_{i,1}, ..., t_{i,m}\}$, for $i = 1, ..., n$. The corresponding n output responses are $\boldsymbol{Y} = \left[(y_1)^T, ..., (y_n)^T\right] \in \mathbb{R}^{mn}$. At this point, the LFGP model is expressed as:

$$\boldsymbol{Y} = \boldsymbol{F}\boldsymbol{\beta} + \boldsymbol{B}\boldsymbol{z} + \boldsymbol{\varepsilon}, \tag{7}$$

Where $\boldsymbol{F} = \left[\boldsymbol{f}_1^T, ..., \boldsymbol{f}_n^T\right]^T$, $\boldsymbol{f}_i = \mathbf{1}_m \otimes \boldsymbol{f}(\boldsymbol{x}_i)^T$, $\mathbf{1}_m$ is an $m \times 1$ column vector with all elements equal to 1, $\boldsymbol{B} = diag\left[\boldsymbol{B}(t_1), ..., \boldsymbol{B}(t_n)\right] \in \mathbb{R}^{mn \times nk}$, $\boldsymbol{B}(\omega_i) = \left[\boldsymbol{b}(t_{i,1}), ..., \boldsymbol{b}(t_{i,m})\right]^T \in \mathbb{R}^{m \times k}$, and $\boldsymbol{\varepsilon}$ is the measurement error. Assuming the latent variables $\boldsymbol{z}$ and measurement errors $\boldsymbol{\varepsilon}$ are mutually independent, $\boldsymbol{Y}$ jointly follows a Gaussian distribution:

$$\boldsymbol{Y} \sim \mathcal{N}\left(\boldsymbol{F}\boldsymbol{\beta}, \sigma^2 \boldsymbol{\Sigma}_y\right), \tag{8}$$

Where $\boldsymbol{\Sigma}_y = \boldsymbol{\Sigma}_b + \delta^2 \boldsymbol{I}_{smn}$, $\boldsymbol{\Sigma}_b = \boldsymbol{B}(\boldsymbol{R} \otimes \boldsymbol{\Sigma}_z)\boldsymbol{B}^T$, and the elements in $\boldsymbol{R}$ and $\boldsymbol{\Sigma}_z$ are calculated by (4) and (5), respectively.

Based on the distribution given in (8), we can derive the log-likelihood function for a given functional response $\boldsymbol{Y}$ as follows:

$$l(\theta, \beta, \sigma^2, \delta^2) = -\frac{1}{2}\left(\log\left|\sigma^2 \boldsymbol{\Sigma}_y\right| + \frac{1}{\sigma^2}(\boldsymbol{Y} - \boldsymbol{F}\boldsymbol{\beta})^T \boldsymbol{\Sigma}_y^{-1}(\boldsymbol{Y} - \boldsymbol{F}\boldsymbol{\beta})\right). \tag{9}$$

Given $\left\{\boldsymbol{\theta}, \delta^2\right\}$, by setting the partial derivative of Equation (9) to 0, we can obtain the estimated values for parameters β and σ^2:

$$\begin{cases} \hat{\boldsymbol{\beta}} = (\boldsymbol{F}^T \boldsymbol{\Sigma}_y^{-1} \boldsymbol{F})^{-1} \boldsymbol{F}^T \boldsymbol{\Sigma}_y^{-1} \boldsymbol{Y} \\ \sigma^2 = \dfrac{1}{mn}(\boldsymbol{Y} - \boldsymbol{F}\hat{\boldsymbol{\beta}})^T \boldsymbol{\Sigma}_y^{-1}(\boldsymbol{Y} - \boldsymbol{F}\hat{\boldsymbol{\beta}}). \end{cases} \tag{10}$$

By substituting the estimated regression parameters $\hat{\boldsymbol{\beta}}$ and variance σ^2 into Equation (9), we can obtain the simplified log-likelihood function:

$$l(\boldsymbol{\theta}, \delta^2) = -\frac{1}{2}(mn \log \sigma^2 + \log\left|\boldsymbol{\Sigma}_y\right|), \tag{11}$$

2.3. Prediction of Functional Response

According to the conditional distribution properties of the Gaussian distribution, the posterior distribution given the training data is still a Gaussian distribution1. After completing parameter estimation, for a new input point $\boldsymbol{x}^*$, the latent variable posterior distribution is [derived from the joint distribution]:

$$\begin{bmatrix} \boldsymbol{Y} \\ \boldsymbol{z}^* \end{bmatrix} \sim \mathcal{N}\left(\begin{bmatrix} \boldsymbol{F}\hat{\boldsymbol{\beta}} \\ 0 \end{bmatrix}, \begin{bmatrix} \hat{\sigma}^2 \boldsymbol{\Sigma}_y & \hat{\sigma}^2 \boldsymbol{C}_{zy}(\boldsymbol{X}, \boldsymbol{x}^*) \\ \hat{\sigma}^2 \boldsymbol{C}_{zy}(\boldsymbol{x}^*, \boldsymbol{X}) & \hat{\sigma}^2 \boldsymbol{\Sigma}_z \end{bmatrix}\right), \tag{12}$$

Where the correlation matrix between $\boldsymbol{Y}$ and $\boldsymbol{z}^*$ is $\boldsymbol{C}_{zy}(\boldsymbol{X}, \boldsymbol{x}^*) = \boldsymbol{B}(\boldsymbol{R}(\boldsymbol{X}, \boldsymbol{x}^*) \otimes \boldsymbol{\Sigma}_z) \in \mathbb{R}^{mn \times k}$.

By deriving the conditional distribution $p(\boldsymbol{z}^* | \boldsymbol{Y})$ from (12), the prediction of $\boldsymbol{z}^*$ can be expressed as:

$$\begin{cases} \hat{\boldsymbol{z}}^* & = \boldsymbol{C}_{zy}(\boldsymbol{x}^*, \boldsymbol{X})\boldsymbol{\Sigma}_y^{-1}(\boldsymbol{Y} - \boldsymbol{F}\hat{\boldsymbol{\beta}}) \\ Cov(\hat{\boldsymbol{z}}^*) & = \hat{\sigma}^2 - \hat{\sigma}^2\boldsymbol{C}_{zy}(\boldsymbol{x}^*, \boldsymbol{X})\boldsymbol{\Sigma}_y^{-1}\boldsymbol{C}_{zy}(\boldsymbol{X}, \boldsymbol{x}^*). \end{cases} \tag{13}$$

In actual modeling, combining the relationship between observed data and B-spline basis functions, and further substituting the estimated values from Equation (13), the prediction for the response $\boldsymbol{y}^* = \left[y(\boldsymbol{x}^*, t_1^*), ..., y(\boldsymbol{x}^*, t_m^*) \right]^T$ at any output location $\boldsymbol{t}^* = \{t_1^*, ..., t_m^*\}$ can be expressed as:

$$\begin{cases} \hat{\boldsymbol{y}}^* & = \boldsymbol{f}^*\hat{\boldsymbol{\beta}} + \boldsymbol{B}(t^*)\hat{\boldsymbol{z}}^* \\ Cov(\hat{\boldsymbol{y}}^*) & = \boldsymbol{B}(t^*)Cov(\hat{\boldsymbol{z}}^*)\boldsymbol{B}(t^*)^T\hat{\sigma}^2\hat{\delta}^2\boldsymbol{I}_m. \end{cases} \tag{14}$$

3. Functional Response Robust Parameter Design Method

3.1. Optimization and Experimental Design

To minimize quality losses caused by product or process fluctuations, we employ an RPD optimization criterion with functional response. Our approach leverages the position effect (i.e., expectation) of the prediction curve for functional response optimization. Specifically, the position effect can be measured using the grey relational degree between the prediction curve and the target curve. The grey relational analysis (GRA) method proposed by Deng Julong in 1982 has been widely applied in the field of optimization [23]. Let the curve of the optimal solution be the target curve $\boldsymbol{y}^0 = \left[y_1^0, y_2^0, ..., y_m^0 \right] \in \square^m$. It can calculate the correlation degree between each position on the prediction curve and the target curve. First, the correlation coefficient for each point is computed using the following formula:

$$\zeta(y_i^*, y_i^0) = \frac{\min\limits_i \left| y_i^* - y_i^0 \right| + \rho \max\limits_i \left| y_i^* - y_i^0 \right|}{\left| y_i^* - y_i^0 \right| + \rho \max\limits_i \left| y_i^* - y_i^0 \right|}, \tag{15}$$

Where y_i^* is the posterior mean given by Equation (14), and ρ is the distinguishing coefficient, typically set to 0.5 by default. The grey relational grade between the predicted curve and the target curve can be obtained by calculating the mean of the relational coefficients for each point.

$$r(\boldsymbol{y}^*, \boldsymbol{y}^0) = \frac{1}{m}\sum_{i=1}^{m}\zeta_i \,. \tag{16}$$

3.2. Functional Response Optimization Model

In this section, the LFGP model is used to obtain the predictive model of the response function with respect to controllable factors. The optimization model constructed from this equation is then optimized to obtain a set of optimal parameters. In this paper, we use a Genetic Algorithm (GA) to optimize the objective function. The genetic algorithm is a heuristic algorithm capable of performing a stochastic global search, which can quickly find the search direction and locate the optimal region. It has the characteristic of global search and can solve global optimization problems. Therefore, a genetic algorithm is used to maximize the objective function. Finally, by selecting the optimal factor levels corresponding to the initial point that maximizes the objective function, the optimization model is constructed as follows:

$$\begin{aligned} &\arg\min Q(\boldsymbol{x}) = \frac{1}{m}\sum_{i=1}^{m}\zeta(E\left[\hat{y}_i(\boldsymbol{x})\right], y_i^0) \\ &s.t. \qquad x \in \square \end{aligned} \tag{17}$$

The Genetic Algorithm (GA) is a heuristic algorithm inspired by biological evolution, proposed by John Holland [24] in 1975. It simulates the mechanisms of selection, crossover (recombination), and mutation found in nature, finding the optimal solution through iterative evolution. Genetic algorithms are particularly suitable for complex non-linear optimization problems and can quickly find the search direction to locate the optimal region. Therefore, GA is used to maximize the objective function. Finally, selecting the optimal factor levels corresponding to the initial point that maximizes the objective function yields a set of optimal parameters x^*.

The basic flowchart of the robust parameter design method proposed in this paper is shown in Figure 1. The implementation process is summarized as follows:

Step 1: Design experiments, then execute the designed experiments and collect stress-strain curves.

Step 2: Standardize the stress-strain curves to facilitate the establishment of the LFGP model.

Step 3: Establish the relationship between input and output of the transformed data using the LFGP modeling method introduced in Section 2.2. Generate the predicted distribution using Equation 2.4 and calculate the predicted mean.

Step 4: Construct a function response optimization model that accounts for position effects.

Step 5: Employ a genetic optimization algorithm to obtain the optimal parameter values that maximize the objective function.

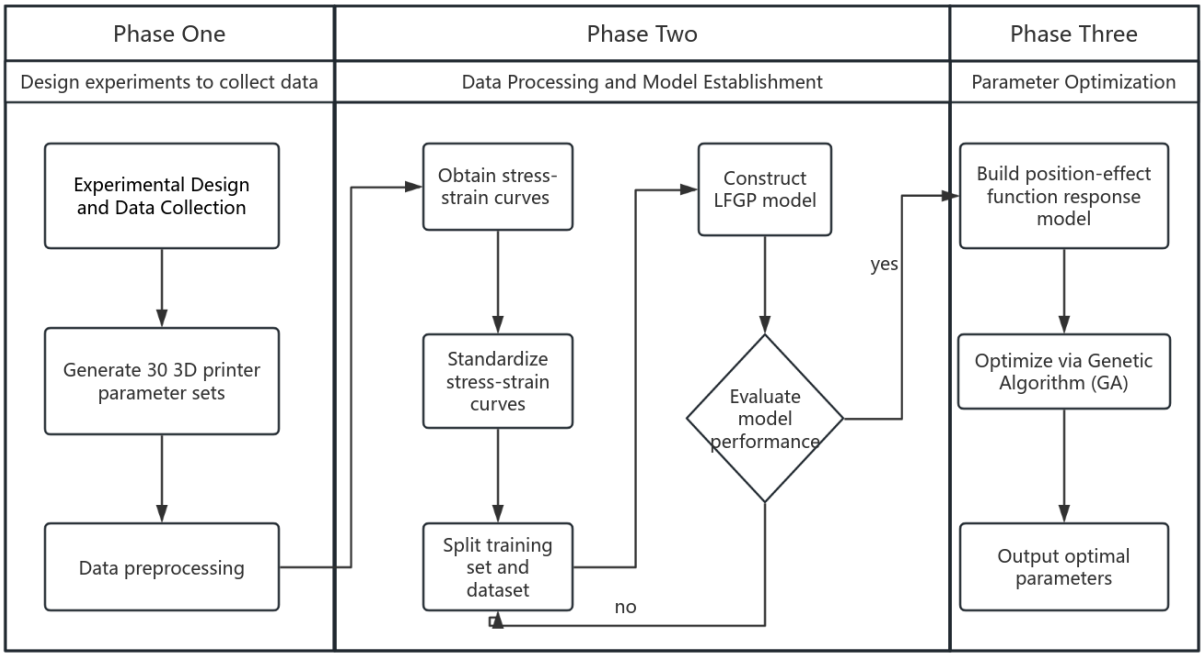

Figure 1. Flowchart of Robust Parameter Design Based on LFGP

4. Additive Manufacturing Case Study

4.1. Experiment Background

All data were sourced from the 3D printing cubic specimen compression performance test at the Jiangsu Provincial Engineering Research Center for High-End Equipment Quality Improvement. In this study, Polymaker's 1.75 mm diameter PolyTerra PLA filament was selected as the printing material. Two dual-nozzle 3D printers (model: FlashForge® Creator 3) were used to print cubic sample parts with dimensions of 20 mm × 20 mm × 20 mm. The settable process parameters include layer height, infill density, printing speed, printing temperature, etc. In the laboratory, when conducting compression tests on the 3D printed parts, the display data from the universal testing machine showed that each compression output data conformed to the characteristics of functional data.

4.2. Experiment Design and Data Collection

We delved into a large volume of literature concerning the optimization of process parameters. Based on literature analysis and practical experience, this study selected 4 key process parameters: Layer Thickness (L), Printing Speed (P), Temperature (T), and Infill Density (I), while other process parameters and environmental parameters were kept constant. Table 1 details these data. Using these four controllable variables, we used the maximin Latin Hypercube Sampling technique to generate parameter combinations. 30 sets of experimental data were successfully collected. The specific design is shown in Table 2.

Table 1. Process Parameters

Process Parameter	Description	Unit	Lower Limit	Upper Limit
L	Layer Thickness	mm	0.1	0.3
P	Printing Speed	mm/s	60	80
T	Temperature	℃	200	230
I	Infill Density	-	10	30

Table 2. Latin Hypercube Parameter Combinations

Number	L	P	T	I
1	0.2622	24.963	72.467	214.62
2	0.1819	15.865	73.036	217.55
3	0.172	23.179	63.396	224.81
4	0.1046	18.214	70.036	216.29
5	0.129	25.611	66.835	210.47
6	0.2526	24.213	60.608	220.22
7	0.2895	27.402	74.72	209.39
8	0.2299	13.544	64.309	200.76
9	0.1606	17.821	62.466	206.7
10	0.2778	16.59	76.11	213.11
11	0.1526	10.932	70.871	226.98
12	0.1981	19.114	69.304	212.43
13	0.1922	11.722	75.866	203.85
14	0.202	20.422	69.334	228.99

Continued Table 2. Latin Hypercube Parameter Combinations

Number	L	P	T	I
15	0.2823	14.68	60.748	201.51
16	0.1537	10.339	71.782	207.57
17	0.2572	22.278	79.866	229.08
18	0.2165	26.503	73.966	215.8
19	0.1788	29.065	74.54	221.65
20	0.2123	21.416	66.51	211.7
21	0.2232	23.626	61.871	218.31
22	0.2346	26.741	77.149	222.59
23	0.1139	12.574	67.868	223.24
24	0.1403	28.465	65.922	202.01
25	0.2437	16.673	62.939	219.77
26	0.1073	19.707	79.17	225.97
27	0.2719	20.829	78.128	208.36
28	0.1256	13.085	64.702	204.52
29	0.1339	14.299	68.461	205.9
30	0.295	29.419	77.823	227.53

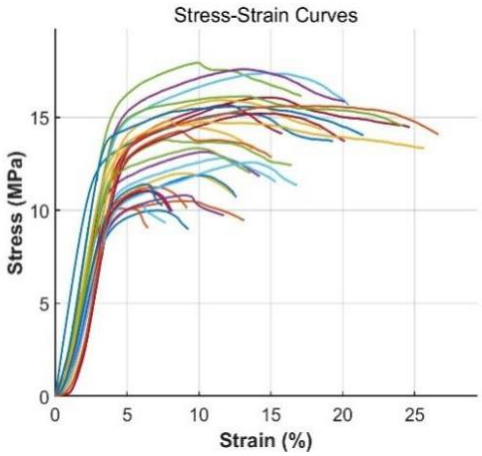

Figure 2 (a). Original Data

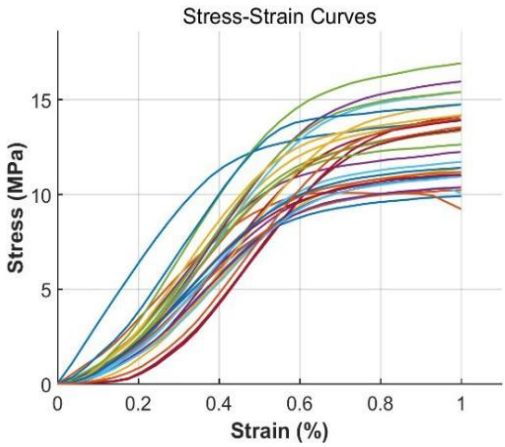

Figure 2 (b). Standardized Data

Based on the experimental design table above, combined with the laboratory's experimental setup, on-site experiments were designed, and 30 sets of stress-strain curves were obtained. In a single compression test, thousands of time points of stress-strain data were recorded, as shown in Figure 2(a). Considering that the length of each stress-strain curve showed non-uniformity, it was difficult to build a model directly. Therefore, a standardization procedure was implemented. As shown in Figure 2(b), each stress-strain curve was transformed into a standard curve composed of 30 time points.

In this section, the selected LFGP model and the Functional Principal Component Regression model (FPCM) are used as baseline models, and the Root Mean Square Error (RMSE) is used to compare the predictive performance of the above models.

$$RMSE = \sqrt{\frac{\sum_{i=1}^{n}\sum_{j=1}^{m}\left(y_i(t_j)-\hat{y}_i(t_j)\right)^2}{mn}} \tag{18}$$

4.3. Experimental Results

To verify the performance of the LFGP model, the first 5 sets of experimental data collected were designated as training data, and the subsequent 25 sets were designated as test data. The training data were used for the model fitting process, while the test data were used to evaluate the model's performance. Here, the Root Mean Square Error (RMSE) serves as the evaluation metric to measure the model's prediction accuracy; a smaller RMSE value indicates superior model performance.

Furthermore, the BK model, BLM model, and FPCM model from the original document were used as baseline methods for comparison. As shown in Figure 3, the proposed LFGP model (RMSE=0.0436) has a lower RMSE value compared to the BK model (RMSE=0.2600), the BLM model (RMSE=1.0581), and the FPCM model (RMSE=0.3384). This clearly indicates that the fitting accuracy of the LFGP model is superior to the three baseline methods. Evidently, this means that in typical cases, the prediction curves generated by the LFGP model have smaller errors, and its predictive performance is superior.

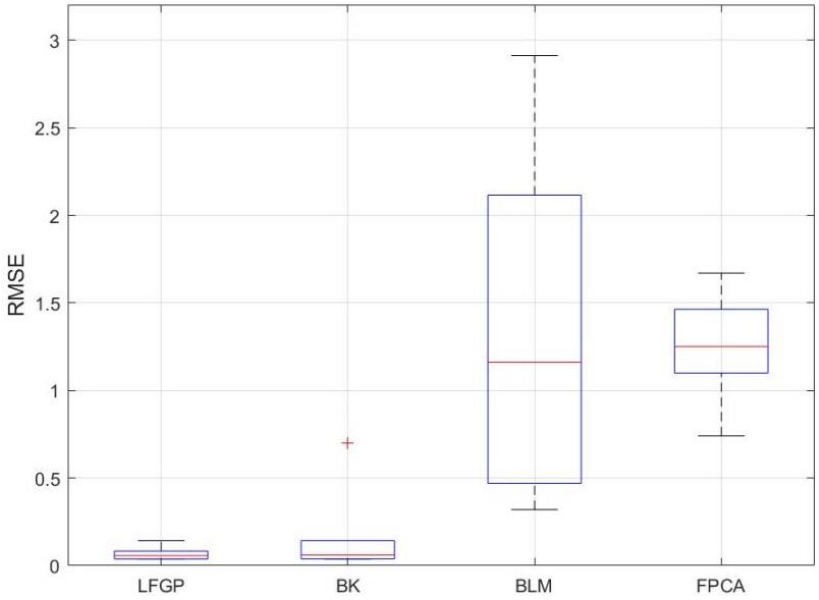

Figure 3. RMSE Results of Different Methods

Following the implementation steps in Section 3.2, we established an optimization model for the experimental data in Figure 2(b). The target curve was constructed from the mean of the training data. The initial settings for the Genetic Algorithm were: parameter lower bound lb = [0.1, 10, 60, 200]; parameter upper bound ub = [0.3, 30, 80, 230]; elite fraction 0.5; population size 500; maximum iterations 100; function value convergence tolerance 1e-6. As shown in Figure 4(a), after converging in 51 iterations, the optimal parameter configuration was obtained. At this time, the Q value of the optimization model was determined to be 0.9765. As shown in Figure 4(b), under such parameter settings, the model's predicted values are highly close to the target values. Specifically, the grey relational grade between the predicted curve and the target curve at this point is 97.65%.

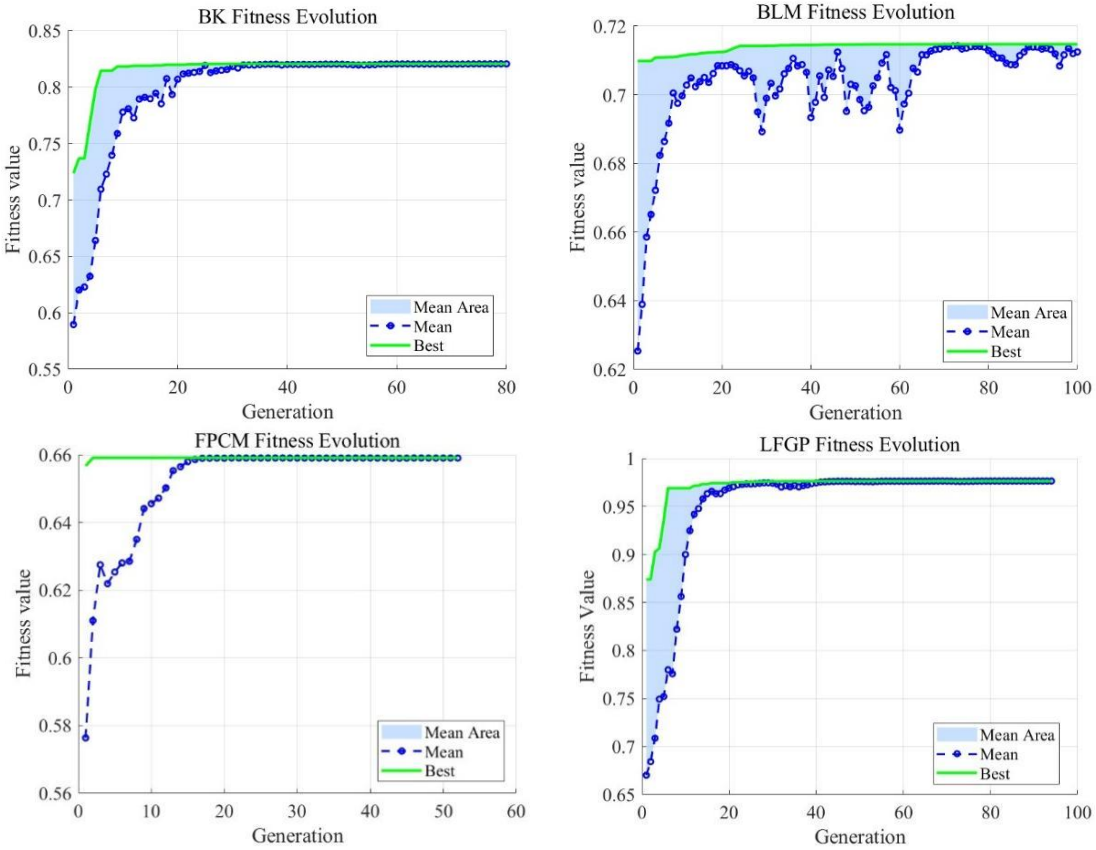

Figure 4. Genetic Algorithm Iteration Plot

Table 3. Comparison of Results

Method	Input Factor Optimization Results				RMSE	Q
	L	P	T	I		
LFGP	0.3000	15.7572	73.6278	226.2604	0.0436	0.9765
FPCM	0.1699	23.7892	75.9493	213.4465	0.3384	0.6585
BK	0.1564	20.6427	80.0000	220.3787	0.2600	0.8216
BLM	0.3000	24.3736	80.0000	211.8926	1.0581	0.6985

As can be seen from Table 3, for the LFGP method proposed in this paper, the optimal parameter configuration obtained after 100 iterations of the genetic algorithm is (L=0.30, I=16, P=73, T=226). At this time, the value of the objective function Q is 0.9765. In contrast, the Q values obtained by the BK, FPCM, and BLM models from the original document are 0.8216, 0.6585, and 0.6985, respectively, all of which are lower than the Q value obtained by the LFGP method in this paper. This result indicates that LFGP is superior to the two-stage methods BLM and FPCM in predicting functional responses. This is because, unlike traditional two-stage methods that need to extract basis functions and eigenvalues from functional data [20,25], LFGP's direct modeling of the raw descriptive data can utilize more functional information, thereby obtaining more accurate predictions. LFGP also shows superior performance to the BK model, which indicates that the non-separable LFBS kernel proposed in LFGP facilitates the transfer of correlation information between different locations of the functional response. In contrast, the separable covariance function used by BK introduces Markov property limitations[26], hindering spatial correlation modeling.

5. Conclusion

This paper addresses the robust parameter design problem for functional responses by proposing a modeling and optimization framework based on a combination of the functional latent Gaussian process (LFGP) and Grey Relational Analysis (GRA). By introducing B-spline basis functions to parameterize the high-dimensional functional response, an LFGP model with a non-separable covariance structure was constructed, effectively capturing the complex dependencies of the functional data between spatial and input variables. An optimization criterion considering the location effect was constructed by combining Grey Relational Grade, and a Genetic Algorithm was employed to achieve global parameter optimization. In the additive manufacturing process parameter optimization case study, the proposed method outperformed traditional two-stage Gaussian process functional regression and principal component analysis methods in terms of prediction accuracy and robustness, validating the superiority of the LFGP model in handling high-dimensional, correlated functional data. The results show that this method can not only significantly improve product quality consistency and process robustness but also provides a generalizable technical path for systems engineering optimization under functional responses. Future research can be further extended to robust optimization under multi-response and multi-working-condition scenarios, and explore Bayesian optimization and active learning strategies based on LFGP to address more complex engineering design and quality control needs.

References

[1] YAN, Jingdong; MA, Shenghua. Research on evaluation of high-end equipment manufacturing achievements from the perspective of scientific and technological achievements transformation. In: International Conference on Education, Management, and Computer. 2019. p. 185 - 194.

[2] TAGUCHI G. Introduction to quality engineering: designing quality into products and processes [M]. 1986.

[3] CHATURVEDI, Saurabh, et al. Evaluation of the methods for determining accuracy of fit and precision of RPD framework in Digital (3D printed, milled) and conventional RPDs-a systematic review. BMC Oral Health, 2024, 24.1: 1466.

[4] Han, M., Ouyang, L. Robust functional response-based metamodel optimization considering both location and dispersion effects for aeronautical airfoil designs. Struct Multidisc Optim 64, 1545 – 1565 (2021).

[5] Marc C. Kennedy, Anthony O'Hagan, Bayesian Calibration of Computer Models, Journal of the Royal Statistical Society Series B: Statistical Methodology, Volume 63, Issue 3, September 2001, Pages 425 – 464

[6] SHI J, WANG B, MURRAY-SMITH R, et al. Gaussian process functional regression modeling for batch data [J]. Biometrics, 2007, 63 (3): 714 - 23.

[7] LIU F, WEST M. A dynamic modelling strategy for Bayesian computer model emulation [J]. 2009.

[8] BAYARRI M J, BERGER J O, KENNEDY M C, et al. Predicting vehicle crashworthiness: Validation of computer models for functional and hierarchical data [J]. Journal of the American Statistical Association, 2009, 104 (487): 929 - 43.

[9] JOSEPH V R, HUNG Y, SUDJIANTO A. Blind kriging: A new method for developing metamodels [J]. 2008.

[10] ROUGIER J. Efficient emulators for multivariate deterministic functions [J]. Journal of Computational and Graphical Statistics, 2008, 17 (4): 827 - 43.

[11] MELKUMYAN A, RAMOS F. Multi-kernel Gaussian processes; proceedings of the IJCAI Proceedings-International Joint Conference on Artificial Intelligence, F, 2011 [C].

[12] LI B, GENTON M G, SHERMAN M. Testing the covariance structure of multivariate random fields [J]. Biometrika, 2008, 95 (4): 813 - 29.

[13] CHUNG S, KONTAR R. Functional principal component analysis for extrapolating multistream longitudinal data [J]. IEEE Transactions on Reliability, 2020, 70 (4): 1321 - 31.

[14] SUNG C-L, WANG W, PLUMLEE M, et al. Multiresolution functional ANOVA for large-scale, many-input computer experiments [J]. Journal of the American Statistical Association, 2020.

[15] CHEN T, HADINOTO K, YAN W, et al. Efficient meta-modelling of complex process simulations with time–space-dependent outputs [J]. Computers & chemical engineering, 2011, 35 (3): 502 - 9.

[16] DEL CASTILLO E, COLOSIMO B M, ALSHRAIDEH H. Bayesian modeling and optimization of functional responses affected by noise factors [J]. Journal of Quality Technology, 2012, 44 (2): 117 - 35.

[17] KONZEN E, CHENG Y, SHI J Q. Gaussian process for functional data analysis: The GPFDA package for R [J]. arXiv preprint arXiv:210200249, 2021.

[18] MA P, MONDAL A, KONOMI B A, et al. Computer model emulation with high-dimensional functional output in large-scale observing system uncertainty experiments [J]. Technometrics, 2022, 64 (1): 65 - 79.

[19] LU J, ZHAN Z, APLEY D W, et al. Uncertainty propagation of frequency response functions using a multi-output Gaussian Process model [J]. Computers & Structures, 2019, 217: 1 - 17.

[20] FANG X, PAYNABAR K, GEBRAEEL N. Multistream sensor fusion-based prognostics model for systems with single failure modes [J]. Reliability Engineering & System Safety, 2017, 159: 322 - 31.

[21] GUO X, JI C, LIU R, et al. A two-stage approach for frequency response modeling and metamaterial rapid design [J]. Progress In Electromagnetics Research C, 2017, 76: 11 - 22.

[22] LIU Z, LI Y, YUE X, et al. Latent functional Gaussian process incorporating output spatial correlations [J]. IISE Transactions, 2024: 1 - 14.

[23] JU-LONG D. Control problems of grey systems [J]. Systems & control letters, 1982, 1 (5): 288 - 94.

[24] HOLLAND J H. Adaptation in natural and artificial systems: an introductory analysis with applications to biology, control, and artificial intelligence [M]. MIT press, 1992.

[25] CAMPBELL K, MCKAY M D, WILLIAMS B J. Sensitivity analysis when model outputs are functions [J]. Reliability Engineering & System Safety, 2006, 91 (10 - 11): 1468 - 72.

[26] O'HAGAN A. A Markov property for covariance structures [J]. Statistics Research Report, 1998, 98 (13): 510.